A Journal of the Gesellschaft Deutscher Chemiker

Angewandte International Edition GDCh Chemie

www.angewandte.org

Accepted Article

Title: HPM-14, a New Germanosilicate Zeolite with Interconnected Extra-Large Pores Plus Odd-Membered and Small Pores

Authors: Zihao Rei Gao, Jian Li, Cong Lin, Alvaro Mayoral, Junliang Sun, and Miguel A. Camblor

To be cited as: *Angew. Chem. Int. Ed.* 10.1002/anie.202011801

Link to VoR: https://doi.org/10.1002/anie.202011801

WILEY-VCH

10.1002/anie.202011801

WILEY-VCH

HPM-14, a New Germanosilicate Zeolite with Interconnected Extra-Large Pores Plus Odd-Membered and Small Pores

Zihao Rei Gao,[a] Jian Li,*[b] Cong Lin,[c,d] Alvaro Mayoral,[e,f,g] Junliang Sun,[c] and Miguel A. Camblor*[a]

[a] Z. R. Gao and Prof. M. A. Camblor
Instituto de Ciencia de Materiales de Madrid, Consejo Superior de Investigaciones Científicas (ICMM-CSIC)
c/ Sor Juana Inés de la Cruz, 3, Madrid, 28049, Spain
E-mail: macamblor@icmm.csic.es
[b] Dr. J. Li
Berzelii Center EXSELENT on Porous Materials, Department of Materials and Environmental Chemistry, Stockholm University, Stockholm, 10691, Sweden
E-mail: jxpxlijian@pku.edu.cn
[c] Dr. C. Lin and Prof. J. Sun
College of Chemistry and Molecular Engineering, Beijing National Laboratory for Molecular Sciences, Peking University
5 Yiheyuan Road, Beijing, 100871, China
[d] Dr. C. Lin
School of Advanced Materials, Peking University, Shenzhen Graduate School, Shenzhen, 518055, China
[e] Dr. A. Mayoral
Instituto de Nanociencia y Materiales de Aragon (INMA-CSIC), Universidad de Zaragoza, 12, Calle de Pedro Cerbuna, 50009 Zaragoza, Spain
[f] Dr. A. Mayoral
Laboratorio de Microscopías Avanzadas (LMA), Universidad de Zaragoza, 50018 Zaragoza, Spain
[g] Dr. A. Mayoral
Center for High-resolution Electron Microscopy (*ChEM*), School of Physical Science and Technology, ShanghaiTech University
393 Middle Huaxia Road, Pudong, Shanghai, 201210, China

Supporting information for this article is given via a link at the end of the document.

Abstract: HPM-14 is a new extra-large pore zeolite synthesized using imidazolium-based organic structure-directing agents, fluoride anions and germanium and silicon as tetrahedral components of the framework. Due to the presence of stacking disorder, the structure elucidation of HPM-14 was challenging, and different techniques were necessary to clarify the details of the structure and to understand the nature of the disorder. The structure has been solved by three-dimensional electron diffraction technique (3D ED) and consists of an intergrowth of two polymorphs possessing a three-dimensional channel system, including an extra-large pore opened through windows made up of sixteen tetrahedral atoms (16-membered ring, 16MR) as well as two additional sets of odd-membered (9MR) and small (8MR) pores. The intergrowth has been studied by scanning transmission electron microscopy (C_s-STEM) and powder X-ray diffraction simulations (DIFFaX), which show a large predominance of the monoclinic polymorph A.

Zeolites continue to attract scientists searching for new structures and applications.[1] While around half a dozen new zeolite framework types are approved each year by the Structure Commission of the International Zeolite Association (SC-IZA),[2] the discovery of new zeolite structures and their structural characterization are still very far from routine. For the discovery, we still rely much on trial and error experiments based on a handful concepts derived from the experience accumulated in the last eight decades or so.[3] The so-called "structure-directing effects", including the use of organic structure-directing agents (OSDA) of various types,[4,5] different mineralizers (fluoride or hydroxide),[6] different heteroatoms (atoms other than Si or Al)[7] and other factors such as concentration of the synthesis mixture,[8] can be used in the design of synthesis experiments aimed to obtaining new zeolites.[9] Among the known zeolites, extra-large pores (*i.e.* pores opened through windows made up of more than 12 tetrahedra) and odd-membered pores are still relatively rare, and very scarcely combined: only two interrupted frameworks (**-IRY** and ***-EWT**),[10] and one true, *i.e.* non-interrupted zeolite framework (GeZA, still to be approved by the SC-IZA)[11] combine large and odd pores. For the structure elucidation, new techniques, especially electron crystallography techniques,[12] have been developed lately that are proving extremely useful in extracting and processing single-crystal-like information from very tiny crystallites, even for impure powder samples. However, materials with structural disorder, such as stacking faults, are particularly difficult to elucidate in all their details and often require combining different techniques. Zeolite beta is a famous case in which electron diffraction (ED) patterns and high-resolution transmission electron microscopy (HRTEM) images were used complementarily to construct possible models. These models were then validated by simulating the corresponding powder X-ray diffraction (PXRD) patterns.[13] The program DIFFaX, which is now regularly used to simulate PXRD patterns of structural models containing stacking faults, was initially developed to characterize zeolite beta.[14] Here, we present HPM-14, a new, fully connected zeolite with extra-large 16MR pores plus additional odd-membered 9MR and small 8MR pores, whose synthesis is based on the combined use of imidazolium-based organic structure-directing agents, fluoride anions and germanium together with silicon as fundamental tetrahedral atoms. While germanosilicate zeolites are generally unstable for high Ge fractions, Ge_f = Ge/(Ge + Si), the discovery of a zeolite with an unusual pore system including large pores may be of fundamental as well as of practical value. Unstable Ge-zeolites may lead to stable zeolites by post-synthesis enrichment in Si.[15] Additionally, unstable Ge-silicate zeolites may lead to stable new materials with new topologies, as shown by the ADOR method,[16] although the abundance of *d4r*, *i.e.* double 4 membered-ring, in HPM-14 would likely make this challenging. Additionally, an interesting zeolite may be targeted by direct synthesis in silica rich form by novel approaches, including the *de novo* design of a more specific OSDA.[17] Because it consists

of an intergrowth of two polymorphs, the structure of HPM-14 was solved by 3D ED methods and the nature of disorder was studied by spherical aberration corrected scanning transmission electron microscopy (C_s-STEM) and powder X-ray diffraction simulations (DIFFaX), which show a large predominance of one of the polymorphs, the monoclinic polymorph A.

For the discovery of HPM-14, two easily synthesized OSDAs (Scheme S1) and a series of high-throughput experiments were performed. With OSDA1, *i.e.* 1-methyl-3-(2',4',6'-trimethylbenzyl)imidazolium, pure zeolite HPM-14 could be synthesized from a gel with composition 0.3 SiO_2 : 0.7 GeO_2 : 0.8 OSDAOH : 0.8 HF : 10 H_2O under rotation at 160 ºC for 4 days (Entry 18b, Tab. S1). OSDA2, *i.e.* 1,1'-((2,4,6-trimethyl-1,3-phenylene)bis(methylene))bis(3-methylimidazolium), was also studied under a more limited range of conditions, yielding pure HPM-14 from a gel composition 0.3 SiO_2 : 0.7 GeO_2 : 0.4 $OSDA(OH)_2$: 0.8 HF : 5 H_2O under rotation at 160 ºC for 7 days (Entries 48c, Tab. S2). Further synthesis details and an account of the influence of several synthesis parameters (time, water content, Ge_f and OSDA/T) on the phase selectivity of the crystallization are described in Section S1 in the Supporting Information (SI). Although HPM-14 has been synthesized using OSDA1 from a relatively wide range of Ge_f (0.3-0.8), the Ge_f range in the synthesized zeolites is notably narrower (0.5-0.7, more frequently 0.6-0.7). An optimum Ge_f in the gel (0.7) affords the synthesis of pure HPM-14 with the same Ge_f in the zeolite while materials prepared from lower or higher Ge_f always present an amorphous Si-rich phase (measured Ge_f < 0.22) or quartz-like GeO_2 impurities, respectively (see Sections S6 and S8). With OSDA2 HPM-14 requires a higher Ge_f in the gel (> 0.5) and produces a zeolite richer in germanium (Ge_f = 0.7-0.8). A thorough characterization of HPM-14 can be found in the SI.

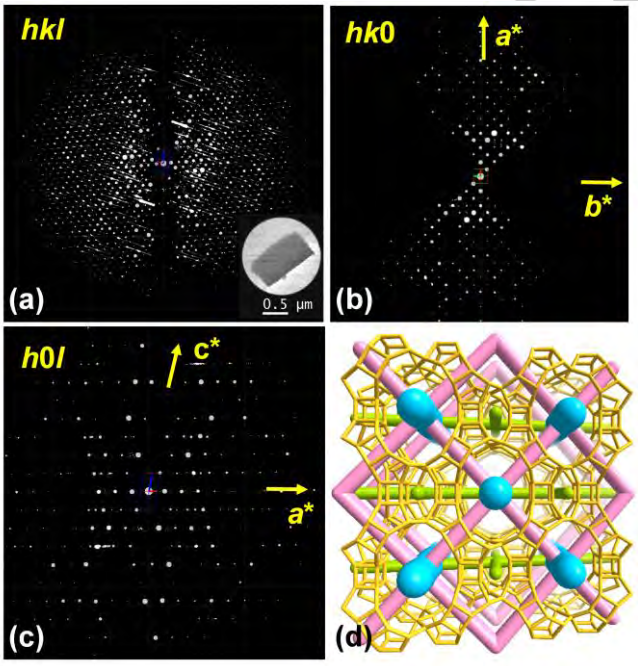

Figure 1. Reconstructed 3D cRED data of HPM-14 indexed with monoclinic symmetry: (a) overview, and selected planes in the reciprocal lattice corresponding to (b) *hk*0 and (c) *h*0*l*. Owing to the streak along *a** for *hkl*: *l* = 2*n* + 1 reflections, some reflections violate the reflection conditions deduced (see text); (d) The multichannel system in HPM-14: one 16MR (blue), two 8MR (green) and two 9MR (pink).

Continuous rotation electron diffraction (cRED) data of as-made HPM-14 from both OSDA1 and OSDA2 were collected and the 3D reciprocal lattice from these two samples were similar, which confirmed that the two OSDA, despite their much different size and shape, were able to direct to the same zeolite structure. One of the typical cRED datasets was directly indexed in a monoclinic unit cell: 23.57 Å, 24.35 Å, 10.51 Å, 90.09º, 100.78º, 90.26º (Figure 1a), *i.e.* $\alpha = \gamma = 90º$ within experimental error. From the 2D slices cut from the 3D reciprocal lattice, we could deduce the reflection conditions to be *hk*0: *h* + *k* = 2*n*, *h*0*l*: *h* = 2*n*, *h*00: *h* = 2*n* (Figure 1b, 1c). Three space groups, *C*2, *Cm*, *C*2/*m*, were found possible after analysis of the reflection conditions. Considering that most zeolite frameworks in the Database of Zeolite Structures are centrosymmetric,[2] the cRED data was processed with fixed unit cell and symmetry *C*2/*m* (the highest symmetry) using XDS program.[18] The monoclinic structure model of HPM-14 (named HPM-14A) was then solved from cRED data by using the dual-space algorithm of ShelxT.[19] 10 unique T atoms (T = Si, Ge) and 23 unique O atoms could be located directly.

However, there were a lot of streaks along *a** axis for *hkl*: *l* = 2*n* + 1 reflections in all the reconstructed 3D reciprocal lattice, which strongly suggested the existence of stacking faults. The typical ED patterns under different tilt angle during cRED data collection confirmed the stacking faults (Fig. S1). After removing the streaks in 3D reciprocal lattice (Fig. S2a-b), an orthorhombic unit cell, with 24.26 Å, 10.49 Å, 23.98 Å, 90.72º, 90.22º, 90.08º ($\alpha = \beta = \gamma = 90º$ within experimental error) can be obtained. The new 2D slices based on the orthorhombic symmetry were cut from the 3D reciprocal lattice using REDp, which suggested possible space group *P*2*na* and *Pmna* (reflection condition: *h*0*l*: *h* + *l* = 2*n*, *hk*0: *h* = 2*n*; Fig. S2c-d). Then, the cRED data were re-processed with the orthorhombic unit cell and symmetry *Pmna* using XDS program again. The orthorhombic structure model of HPM-14 (HPM-14B) was outputted with the same number of unique T atoms and O atoms as HPM-14A by ShelxT. In order to facilitate the description of the structure of HPM-14A and HPM-14B, we rearranged the unit cell parameters of HPM-14B with non-standard space group *Pbmn* (Permutation: *c*, *a*, *b*). Then, the unit cell parameters were refined by Lebail fitting of the powder diffraction data of a calcined sample, which resulted in 23.0100(6) Å, 24.1426(8) Å, 10.3774(8) Å, 90º, 99.878(5)º, 90º for HPM-14A (Fig. S3), and 22.6690 Å, 24.0884 Å, 10.6490 Å, 90º, 90º, 90º for HPM-14B (Fig. S4). Finally, the frameworks of HPM-14 synthesized with OSDA1 and OSDA2 were refined against the cRED data. CIF files and futher details can be found in SI (Section S7 and Tab. S3).

The channel system of HPM-14 is 3D with intersecting 16+8 × 9+8 × 9 MR. The 16MR and one of the 8MR channels are 1D along [001] direction (Figure 1d). These are connected in the perpendicular directions through 9MR windows forming a 2D undulating channel and through 8MR windows forming a 1D straight channel. This results into an interconnected 3D pore system with pore apertures of 12.3×8.6 Å (16MR), 5.6×3.7 Å (9MR), 5.4×1.9 Å (8MR along *c*-axis), and 4.6×3.9 Å (8MR along *a*-axis), respectively (Fig. S5). The stacking faults do not fundamentally affect the porosity of HPM-14. Argon adsorption analysis on a calcined HPM-14 sample shows maxima at 5.9 and 12.5 Å in the pore size distribution derived by DFT (Fig. S6), which matches well with the porosity system determined by crystallography.

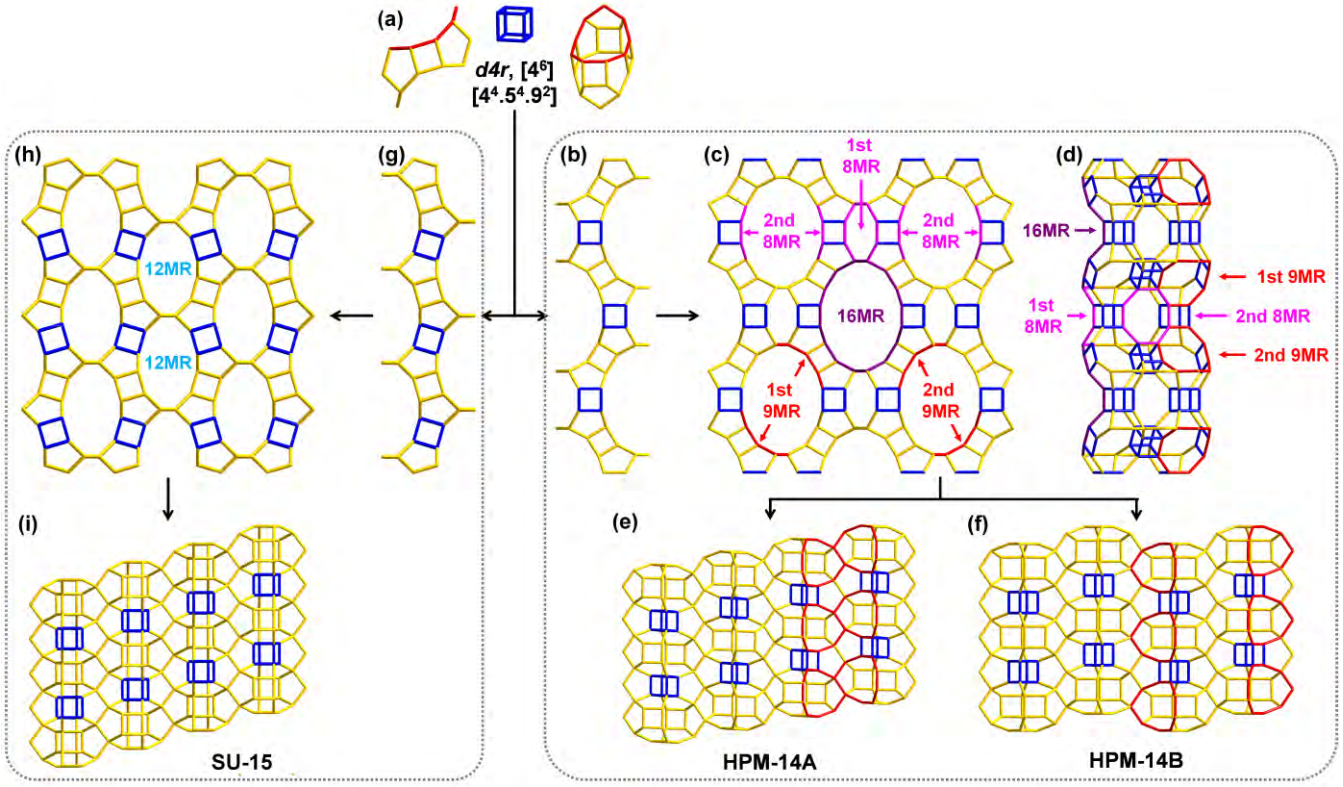

Figure 2. Structure description of HPM-14 and **SOF**: (a) *d4r* and [$4^4.5^6.9^2$] tiles, (b) HPM-14-chain formed by mirror plane operation, (c) HPM-14-layer along [001], (d) two consecutive HPM-14-chains showing the 9 and 8 MR pores running in the plane normal to [001], (e) HPM-14A along [010], showing AAAA packing, (f) HPM-14B along [010], showing ABAB packing, (g) **SOF**-chain formed by an inversion symmetry operation, (h) **SOF**-layer along [001], and (i) **SOF** along [010], showing AAAA packing. Only T-atom connections are shown; highlighted T-atoms: violet (16MR), red (9MR), pink (8MR) and blue (*d4r*).

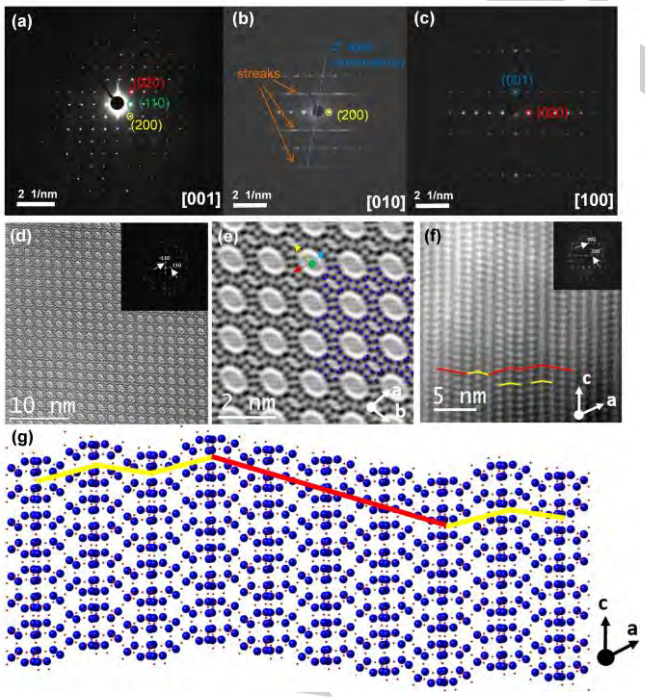

Figure 3. C_s-corrected STEM analysis of HPM-14. SAED patterns along (a) [001], (b) [010] showing diffuse streaks, (c) [100]. (d) ABF high-resolution image of the framework along [001]. (e) A closer look allows the visualization of the extra-large pores (green dot) and smaller rings (marked by yellow, red and blue arrows for 8, 5 and 4 MRs, respectively). (f) High-resolution micrograph along [010]. (g) Schematic model with the Si and O (blue and red spheres, respectively). In (d) and (f), the FD is presented in the inset; in (f) and (g) the stacking sequence has been marked with red and yellow lines denoting monoclinic and orthorhombic domains, respectively. The regions where both polymorphs coexist are marked by red and yellow lines at different position heights.

The framework of HPM-14 shows some similarity but significant differences to the **SOF** framework (SU-15 zeolite).[20] Both structures have the *t-sof*-2, *i.e.* [$4^4.5^6.9^2$] and the *d4r*, *i.e.* [4^6] (Figure 2a) tiles and may be built using a chain that contains the [$4^4.5^6.9^2$] tiles. However, neighboring [$4^4.5^6.9^2$] tiles are related by an inversion point in **SOF**-chain (Figure 2g) and by a mirror plane in HPM-14-chain (Figure 2b). This converts the 12MR channel in **SOF** into a 16MR plus an 8MR channel in HPM-14. Then, HPM-14-layers (Figure 2c) and **SOF**-layers (Figure 2h) are formed by connection of consecutive HPM-14-chains or **SOF**-chains, related by a glide plane, along the [100] direction. Successive layers are connected by *d4r*s to form the 3D framework of HPM-14 or **SOF**.

The differences between HPM-14A and HPM-14B are related to the way successive chains are connected along the *a*-axis. When chains connect always at the same side an AAAA packing results in the monoclinic HPM-14A (Figure 2e), while connecting at alternating sides yields the ABAB packing of the

orthorhombic HPM-14B (Figure 2f). The packing of HPM-14A is similar to that of **SOF** (Figure 2i), also monoclinic. We predict that, similar to HPM-14, an orthorhombic variant of **SOF** might exist, although there are no signs of intergrowths in the actual SU-15 zeolite.[20]

The stacking faults described are fully supported by selected area electron diffraction (SAED) data, which show diffuse scattering patterns in the low-order zone axis more clearly than the cRED data. SAED patterns along the [010] direction show that all reflections with $l = 2n$ are sharp (Figure 3b), while reflections with $l = 2n + 1$ appear as streaks along a^* direction. This indicates stacking disorder along the direction parallel to a^* with a translation of layers by ±1/2*c*. The absence of streaks along [100] and [001] (Figure 3a, 3c), indicates that there is no disorder in the projection along the *a*- and *c*- axes.

Electron Microscopy analysis was performed by means of spherical aberration corrected (C_s-corrected) Scanning Transmission Electron Microscopy (STEM) with an annular dark field/bright field detector (ADF/ABF). Figure 3d displays the C_s-corrected STEM-ABF image along the [001] orientation, where the oval shaped large pores are clearly visualized. The Fourier diffractogram (FD, inset) can be indexed in the *C2/m* space group. A closer inspection of the framework (Figure 3e) allows the visualization of the 16MRs surrounded by 8, 5 and 4 MRs. On a crystal rotated 90° with respect to the [001] direction the existence of a disordered structure is evidenced (Figure 3f). The resulting structure is predominantly monoclinic. A schematic model representing the existence of these stacking faults is depicted in Figure 3g.

Fig. S7 and S8 show the DIFFaX simulations of intergrown structures together with the experimental pattern of calcined HPM-14 (see SI for further details and discussion). The comparison reveals that HPM-14 is predominantly the monoclinic polymorph A, with around 85-90% predominance. The major presence of HPM-14A is also proved by C_s-corrected STEM images (Fig. S9).

In conclusion, HPM-14 is a new germanosilicate zeolite with a three-dimensional system of pores including extra-large 16MR pores of 12.3×8.6 Å free aperture. These, together with small 8MR pores, run along [001] direction, while in the perpendicular direction 8MR and 9MR pores exist. The zeolite was synthesized using two different types of imidazolium cations (one monocationic, the other dicationic) of facile synthesis. The structure, which has a very low framework density of 14.1 T/1000 Å^3, was solved by cRED which evidenced the existence of two intergrown polymorphs, one monoclinic (HPM-14A), the other orthorhombic (HPM-14B), due to stacking faults along [100] direction. The stacking faults do not block the extra-large pore and have little impact on the smaller pores that connect them, because the large pores are separated from each other by very small stretches of 8MR and 9MR pores. The intergrowth has been studied by C_s corrected STEM and DIFFaX simulations of the XRD patterns, concluding a large predominance of the monoclinic polymorph HPM-14A.

Acknowledgements

The authors acknowledge financial support by the Spanish Ministry of Science, Innovation and Universities (MAT2015-71117-R and PID2019-105479RB-I00 projects, AEI, Spain and FEDER, EU), the National Natural Science Foundation of China (No. 21871009, 21621061, 21527803, 21471009, NFSC-21850410448, NSFC-21835002), the Swedish Research Council (VR) and the Knut and Alice Wallenberg Foundation (KAW), and the Centre for High-resolution Electron Microscopy (ChEM), supported by SPST of ShanghaiTech University under contract No. EM02161943. A.M. also acknowledges funding by the Spanish Ministry of Science, Innovation and Universities through the Ramon y Cajal Program (RYC2018-024561-I).

Keywords: zeolites • extra-large pores • structure solution • three-dimensional electron diffraction • stacking faults

[1] a) A. Burton, *Catal. Rev. Sci. Eng.* **2018**, *60*, *1*, 132-175; b) J. Shin, D. Jo, S. B. Hong, *Acc. Chem. Res.* **2019**, *52*, *5*, 1419-1427.

[2] Ch. Baerlocher, L. B. McCusker, *Database of Zeolite Structures*: http://www.iza-structure.org/databases/, access on **March 8th, 2020**.

[3] a) C. S. Cundy, P. A. Cox, *Chem. Rev.* **2003**, *103*, 663-702; b) C. S. Cundy, Cox, P. A., *Microporous Mesoporous Mater.* **2005**, *82*,1-78.

[4] R. F. Lobo, S. I. Zones, M. E. Davis, *J. Incl. Phenom. Macrocycl. Chem.* **1995**, *21*, 47-78.

[5] *Insights into the Chemistry of Organic Structure-directing Agents in the Synthesis of Zeolitic Materials*, *Vol. 175* (Eds.: L. Gómez-Hortigüela), Springer, **2018**.

[6] a) E. M. Flanigen, R. L. Patton, *U.S. Patent* 4, 073, 865, **1978**; b) *Hydrothermal Chemistry of Zeolites* (Eds.: R. M. Barrer), Academic Press, London, **1982**.

[7] P. Lu, L. A. Villaescusas, M. A. Camblor, *Chem. Rec.* **2018**, *18*, 1-12.

[8] a) M. A. Camblor, L. A. Villaescusa, M. J. Díaz-Cabañas, *Top. Catal.* **1999**, *9*, 59-76; b) M. A. Camblor, P. A. Barrett, M. J. Díaz-Cabañas, L. A. Villaescusa, M. Puche, T. Boix, E. Perez, H. Koller, *Microporous Mesoporous Mater.* **2001**, *48*, 11-22; c) J. Song, H. Gies, *Stud. Surf. Sci. Catal.* **2004**, *154A*, 295-300; d) S. I. Zones, R. J. Darton, R. Morris, S. J. Hwang, *J. Phys. Chem. B* **2005**, *109*, 652-661.

[9] L. A. Villaescusa, J. Li, Z. Gao, J. Sun, M. A. Camblor, *Angew. Chem.* **2020**, *132*, 11379-11382; *Angew. Chem. Int. Ed.* **2020**, *59*, 11283-11286.

[10] a) A. Corma, M. J. Díaz-Cabañas, J. Jiang, M. Afeworki, D. L. Dorset, S. L. Soled, K. G. Strohmaier, *Proc. Natl. Acad. Sci.* **2010**, *107*, 13997-14002; b) T. Willhammar, A. W. Burton, Y. Yun, J. Sun, M. Afeworki, K. H. Strohmaier, H. Vroman, X. Zou, *J. Am. Chem. Soc.* **2014**, *136*, 13570-13573.

[11] C. Jo, S. Lee, S. J. Cho, R. Ryoo, *Angew. Chem.* **2015**, *127*, 12996-12999; *Angew. Chem. Int. Ed.* **2015**, *54*,12805-12808.

[12] a) W. Wan, J. Sun, J. Su, S. Hovmoller, X. Zou, *J. Appl. Cryst.* **2013**, *46*, 1863-1873; b) J. Li, J. Sun, *Acc. Chem. Res.* **2017**, *50*, *11*, 2737-2745; c) J. Li, C. Lin, Y. Min, Y. Yuan, G. Li, S. Yang, P. Manuel, J. Lin, J. Sun, *J. Am. Chem. Soc.* **2019**, *141*, 4990-4996.

[13] M. M. J. Treacy, J. M. Newsam, M. W. Deem, *Proc. R. Soc. Lond. A* **1991**, *433*, 499-520.

[14] M. M. J. Treacy, M. W. Deem, *DIFFaX. A computer program for calculating Diffraction Intensity from Faulted Crystals*, v. 1.813, **19th May 2010**.

[15] a) H. Xu, J.-G. Jiang, B. Yang, L. Zhang, M. He, P. Wu, *Angew. Chem.* **2014**, *126*, 1379-1383; *Angew. Chem. Int. Ed*. **2014**, *53*, 1355-1359; b) L. Burel, N. Kasian, A. Tuel, *Angew. Chem*. **2014**, *126*, 1384-1387; *Angew. Chem. Int. Ed*. **2014**, *53*, 1360-1363; (c) Z.-H. Gao, F.-J. Chen, L. Xu, L. Sun, Y. Xu, H.-B. Du, *Chem. Euro. J.* **2016**, *22*, 14367-14372.

[16] a) W. J. Roth, P. Nachtigall, R. E. Morris, P. S. Wheatley, V. R. Seymour, S. E. Ashbrook, P. Chlubná, L. Grajciar, M. Položij, A. Zukal, O. Shvets, J. Čejka, *Nature Chem.* **2013**, *5*, 628-633; b) M. Mazur, P. S. Wheatley, M. Navarro, W. J. Roth, M. Položij, A. Mayoral, P. Eliášová, P. Nachtigall, J. Čejka, R. E. Morris, *Nature Chem.* **2016**, *8*, 58-62.

[17] a) D. W. Lewis, D. J. Willock, C. R. A. Catlow, J. M. Thomas, G. J. Hutchings, *Nature* **1996**, *382*, 604-606; b) K. Muraoka, W. Chaikittisilp, T. Okubo, *Chem. Sci*. **2020**, *11*, 8214-8223.
[18] W. Kabsch, *Acta. Cryst. D* **2010**, *66*, 125-132.
[19] G. M. Sheldrick, *Acta. Cryst. A* **2015**, *71(1)*, 3-8.
[20] L. Tang, L. Shi, C. Bonneau, J. Sun, H. Yue, A. Ojuva, B.-L. Lee, M. Kritikos, R. G. Bell, Z. Bacsik, J. Mink, X. Zou, *Nature Mater.* **2008**, *7*, 381-385.

10.1002/anie.202011801

Entry for the Table of Contents

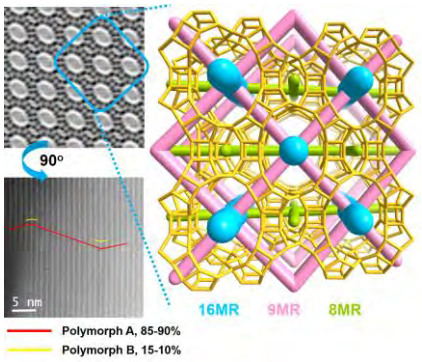

HPM-14 is a new zeolite that combines extra-large pores (12.3×8.6 Å) with odd-membered plus small pores. The presence of stacking faults disorder made unveiling its structural details demanding of a combination of different techniques: rotation electron diffraction, high resolution scanning transmission electron microscopy and powder X-ray diffraction simulations.

Institute and/or researcher Twitter usernames: @icmmcsic, @EMeSax, @zihao_gao